ELSEVIER

Journal of Power Sources 75 (1998) 236–243

JOURNAL OF POWER SOURCES

Direct observation of the oxidation nickel in molten carbonate

Yoshiyuki Izaki [a,*], Yoshihiro Mugikura [a], Takao Watanabe [a], Makoto Kawase [a], J. Robert Selman [b]

[a] *Yokosuka Research Laboratory, Central Research Institute of Electric Power Industry, 2-6-1, Nagasaka, Yokosuka-shi, Kanagawa-ken, 240-01 Japan*
[b] *Department of Chemical and Environmental Engineering, Illinois Institute of Technology, 10W, 33rd St., Chicago, IL 60616, USA*

Received 15 May 1998; accepted 23 May 1998

Abstract

Polarization of the nickel oxide (NiO) cathode limits the performance of the state-of-the-art MCFC. It is therefore important to clarify the phenomena which occur when, as is usually the case, the NiO cathode is formed in situ in the MCFC. This occurs by chemical or electrochemical reactions between nickel, which is the base material of the cathode, and molten carbonate (usually Li_2CO_3:K_2CO_3 = 62:38 mol%), which is the electrolyte. To clarify these formation phenomena, a direct observation method involving a telescope and CCD (charge coupled device) camera, in combination with potential measurements, is applied to the oxidation of a nickel sheet which is partially immersed in molten carbonate. In an atmosphere of pure CO_2, a partially immersed nickel sheet is relatively stable, as is a gold foil even in oxidant gas. In the case of nickel exposed to oxidant gas, however, the area exposed directly to the oxidant gas is rapidly covered by an electrolyte film, and undergoes intensive chemical or electrochemical reactions with CO_2 gas generation during oxidation and lithiation. As a consequence, a progressively rougher NiO surface develops over the entire sheet. After oxidation and lithiation, the non-immersed part of the sheet remains covered with electrolyte. Although the oxygen reduction current at the in situ lithiated NiO is over one order of magnitude higher than that at a gold electrode at the same applied potential, the extended meniscus region is the dominant reaction site for oxygen reduction. The same is true for the much more limited meniscus region of the gold electrode.

Keywords: Direct observation; In situ oxidation; Lithiation; Molten carbonate; Fuel cell; Nickel oxide cathode

1. Introduction

The molten carbonate fuel cell (MCFC) is expected to play an important role in future power-generation systems. Development of the MCFC, carried out in the USA, Japan and Europe [1–3], has reached the stage of large-scale demonstration and several 100 to 1000 kW power plants have been planned or installed. To make MCFC commercialization possible, however, it is important to reduce the initial cost by improving the power density and useful lifetime of the stacks. These improvements on state-of-the-art technology will require significant advances in the basic understanding of MCFC operation [4,5].

In spite of sustained research efforts during recent years, several important phenomena which take place in the MCFC are still not completely understood. Polarization of the cathode limits the performance of the state-of-the-art MCFC [6,7]. To improve the energy density, it is necessary to optimize the electrode structure, since the cathode reactions of the MCFC take place in porous electrodes. Such porous electrodes must contain electrolyte but should not be completely filled. The extent of the reaction zone in these electrode is not known. It depends, of course, on the particle size and porosity of the lithiated NiO that is presently used as the cathode material. This material is generally formed by in situ oxidation of nickel particles which are contained in the cathode space of cells/stacks.

In the state-of-the-art MCFC, the final structure of cathode (lithiated NiO) is determined by the in situ oxidation/lithiation process. The latter usually takes place as a district phase during the heating-up of the cold-assembled cell or stack. MCFC developers may use different operating conditions during this in situ cathode-formation process, i.e., cathode gas composition, temperature and process duration (or alternatively a prescribed temperature programme). The conditions are usually based on exten-

* Corresponding author. Tel.: +81-468-56-21-21; Fax: +81-468-56-33-46; E-mail: izaki@yokosuka.denken.or.jp

0378-7753/98/$19.00
PII: S0378-7753(98)00117-7

sive experience with small single cells, but the optimum cathode-formation conditions in large-scale stacks may still be difficult to achieve. The most important factor to be controlled appears to be the temperature, since the in situ oxidation process is strongly exothermic. Therefore, the gas composition and flow rate are controlled such that the maximum temperature reached during the process remains below a maximum value, which has been determined empirically. In many cases, this appears to imply that very low oxygen partial pressures must be used. The optimal rate for the in situ process must depend, however, on the stack configuration and scale. Very little is known about the relationship between formation conditions and cathode electrode structure. This work aims to make a contribution to the understanding of the in situ cathode-formation process.

As a first step, phenomena involving the electrode/gas/electrolyte interface in the MCFC cathode, such as wetting and de-wetting [8–14], must be clarified. For optimal design of the cathode structure, it is essential to elucidate the interaction between nickel metal and molten carbonate under MCFC operating conditions, including cathode pretreatment conditions [15,16]. This interaction determines what happens in the later stages of the in situ process and, thereby, the extent of the reaction area in the porous cathode ('conditioning' of the electrode).

An actual porous electrode is very difficult to use for observation of the in situ process, because of many uncontrollable factors. Thus, in order to gain insight into the behaviour of the three-phase boundary in a molten carbonate electrode, partially-immersed gold and nickel foils were used in this work. Gold was selected because it is stable in molten carbonate even under oxidizing (cathode gas) conditions. A few investigations of the corrosion of nickel metal partially immersed in molten carbonate have been reported, but the chosen experimental conditions and electrolyte were very different to those used in the state-of-the-art MCFC [17].

This study deals in particular with surface changes of the nickel foil during in situ oxidation and lithiation. The objective is to elucidate the electrolyte behaviour in these processes by means of direct observation of the sample. The electrochemical performance of an in situ lithiated NiO electrode is also examined, and compared with that of a meniscus-type electrode formed by a gold foil partially immersed in molten carbonate. The aim is to estimate and compare the extent of reaction in these two types of electrode.

2. Experimental

A schematic of the experimental equipment is shown in Fig. 1. The system consists of four main parts, namely, an electric furnace, electrochemical measurement equipment, optical observation equipment, and a gas-supply unit.

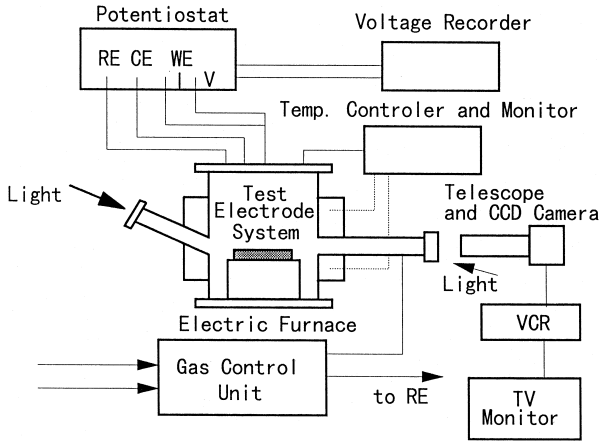

Fig. 1. Experimental set-up.

The electric furnace (made by Applied Test Systems, USA) has two electric heaters controlled by two temperature controllers (Model CN9000, Omega, USA), and a cylindrical stainless-steel container with two windows for optical observation. The electrochemical measurement equipment consists of a potentiostat (Standard Potentiostat Wenking, model ST 72, Gerhard Bank Elektronik, Germany), a multimeter (Type 8062A, Fluke, USA) for measurement of electrode potential, and a portable recorder (Type 3057, Yew, Japan) for measurement of the current through the electrode. The optical equipment consists of a telescope (Monozoom 7, Bausch & Lomb, USA), a CCD (charge couple device) video camera (Model VDC 3800, Sanyo, Japan), and a TV monitor (Model No. BWM9A, Javelin Electronic, USA). The gas-supply units has two flow meters (Model FL-3845G and FL-3845C, Omega, USA), two gas-drying columns (W.A. Hammond Drierie, USA), and associated valves.

The test electrode system is located in the centre of the furnace. A schematic of the electrode system is shown in Fig. 2. The working electrode (WE) is a gold foil ($25 \times 25 \times 0.125$ mm^3) or a nickel sheet ($25 \times 25 \times 0.5$, 0.25 mm)

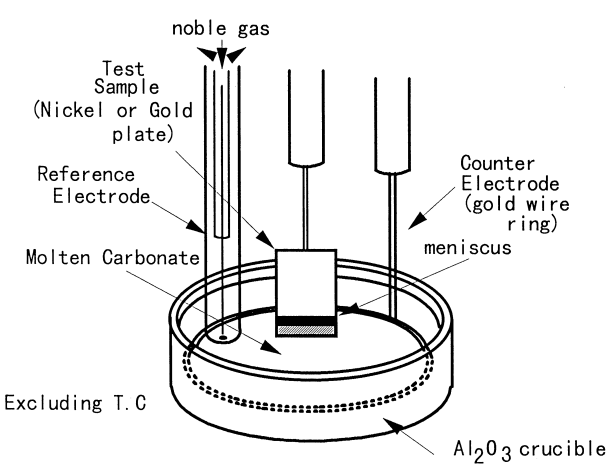

Fig. 2. Electrode configuration in test cell.

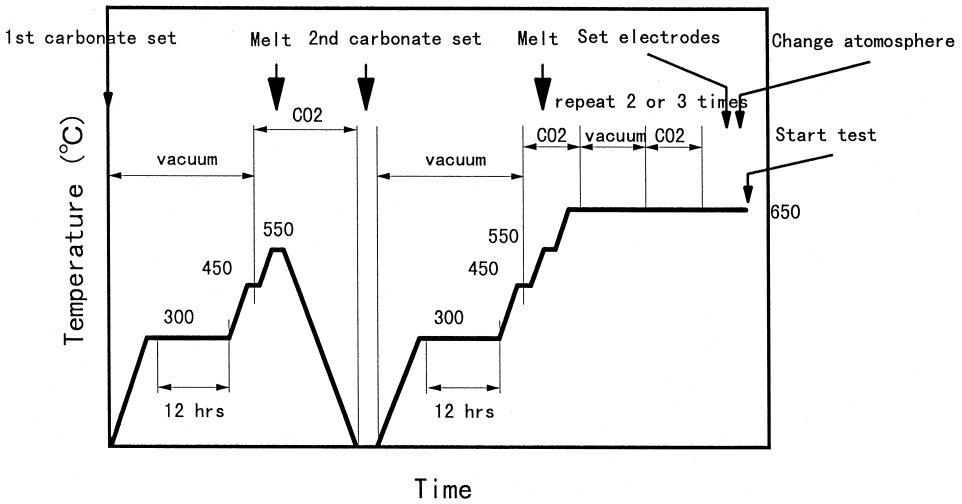

Fig. 3. Experimental procedure.

with a gold wire (diameter 1 mm) as a current lead. The reference electrode (RE) is a partially coiled gold wire of diameter 0.5 mm. The counter electrode (CE) is a coiled gold wire of diameter 1 mm. All electrodes and ceramic components were rinsed with a solvent, to remove organic compounds, and with acid solution.

The eutectic carbonate (Li_2CO_3:K_2CO_3 = 62:38 mol%) was melted in the ceramic dish (diameter 60 mm, height 20 mm, made of AD-998 aluminum oxide by Coors) in two batches so as to fill completely the dish with electrolyte. After the first electrolyte batch was inserted in the furnace, heating was started according to the procedure shown in Fig. 3. Before the second batch melted, the electrodes were assembled and inserted in the furnace. After the electrolyte had melted and its temperature reached 650°C, the counter and reference electrodes were immersed in the melt. As soon as the RE had been immersed, reference gas (O_2:CO_2 = 33:67 mol%) was supplied to prevent plugging of the gas channels in the electrode by the electrolyte. Finally, the WE was partially immersed in the electrolyte, and the experimental gas (O_2:CO_2:N_2 = 15:30:55 mol% or pure CO_2) was supplied to the furnace.

3. Results and discussion

3.1. Studies of meniscus formed by molten carbonate at a gold electrode

In this experiment, the cross-section of the meniscus was observed directly via a telescope. Although the geometry of the meniscus could not be measured completely due to focusing imperfections, it was confirmed that the contact angle at a gold electrode is approximately 60°. A clear demarcation between the electrode and the electrolyte was discernible, as shown in Fig. 4. A super-meniscus film could not be observed on gold even in the oxidant gas atmosphere.

To characterize the meniscus system and to determine the reaction site, the current at a controlled cathodic potential was measured at different depths of immersion of the WE. The effect of the immersed depth on the current is shown in Fig. 5. The influence on the current becomes less as the immersed depth is increased. At a depth of more than 10 mm, the current becomes largely independent of the depth. This indicates that the meniscus region is the dominant reaction zone for oxygen reduction at a gold electrode partially immersed in molten carbonate [16]. The magnitude of the linear current density is in the range 0.02 to 0.03 mA cm^{-1} at −200 mV.

3.2. Wetting and oxidation of nickel metal by molten carbonate

3.2.1. Pure CO_2 atmosphere

A nickel sheet ($25 \times 25 \times 0.5$ mm^3) was partially immersed in Li–K eutectic carbonate in an atmosphere of pure CO_2. The meniscus could be observed clearly and, initially, a super-meniscus film was not discernible, as in the case of gold foil. This initial observation period lasted

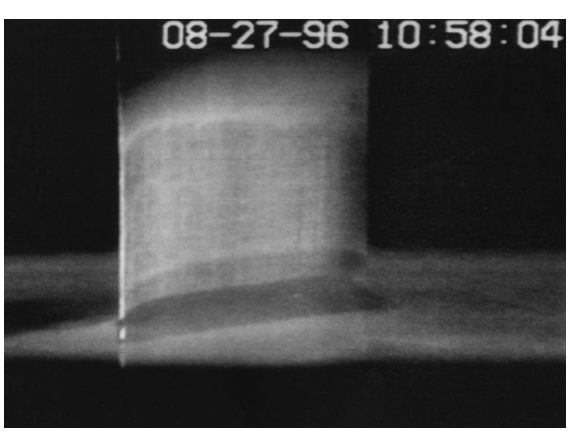

Fig. 4. View of the meniscus on a gold electrode.

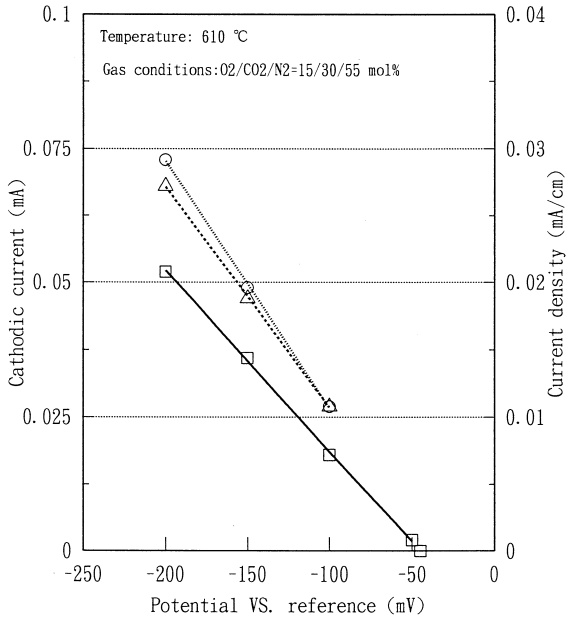

Fig. 5. Effect of immersed depth of gold cathode on current/potential. Depth: (– □ –) 5 mm; (· · · △ · · ·) 10 mm; (· · · ○ · · ·) 15 mm.

for more than 2 h. During this period, the contact angle between the nickel sheet and the electrolyte was constant ($\sim 50°$), as was the potential between the nickel sheet and the reference electrode, viz., −758 mV. This value corresponds to the equilibrium potential of nickel oxidation in molten carbonate:

$$Ni + CO_3^{2-} \rightarrow NiO + CO_2 + 2e^- \quad (1)$$

3.2.2. Oxidant gas atmosphere

After observation of the nickel sheet in pure CO_2, an oxidant gas mixture (O_2:CO_2:N_2 = 15:30:55 mol%) was supplied. The change in potential of the nickel electrode as a function of time is presented in Fig. 6. As soon as the gas mixture including oxygen was supplied, the potential began to shift to more positive values. Simultaneously, it was observed that the surface of the non-immersed part of the sheet became cloudy and the potential rapidly shifted further. Gas evolution started to take place from the immersed part of the sheet, and a vapour mist (or spray) rose from the surface of the electrolyte. Some of this vapour seemed to condense or adsorb on the electrode surface. These phenomena were observed approximately 1 h after supplying the gas mixture.

When the nickel sheet was rotated to facilitate observation of its surface, it became evident that after approximately 1 h the surface of the non-immersed part of the sheet had become covered with electrolyte and that a reaction accompanied by gas generation was taking place. Meanwhile, the potential gradually shifted to more positive values. After about 4 h, the potential curve reached a plateau at about −470 mV, which persisted for about 17 h, while the surface reaction continued. The phenomena on the non-immersed part of the sheet are illustrated in Fig. 7.

The first plateau was ended by an abrupt potential drop of about 100 mV, followed again by a gradual shift to more positive values. Simultaneously, the exposed (non-immersed) part of the electrode started to show delamination (cleavage). After about 50 h, the potential reached a second plateau at approximately −220 to −230 mV. During passage through this plateau, many corrosion products accumulated on the nickel sheet and some were observed in the electrolyte bath. Corrosion products also tended to move on to the surface of the ceramic components. Towards the end of the second plateau, it appeared that the reaction taking place on the non-immersed electrode surface had ceased but gas bubbles were still rising from the immersed part of the sheet.

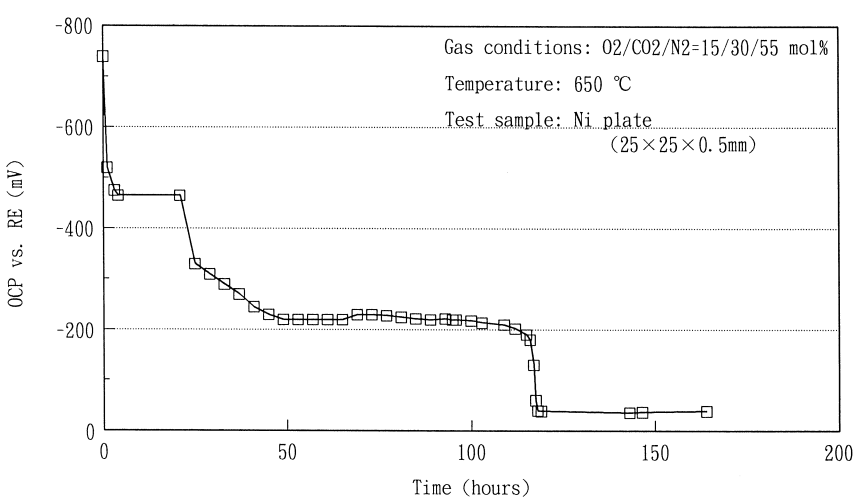

Fig. 6. Potential history of nickel sheet during oxidation/lithiation.

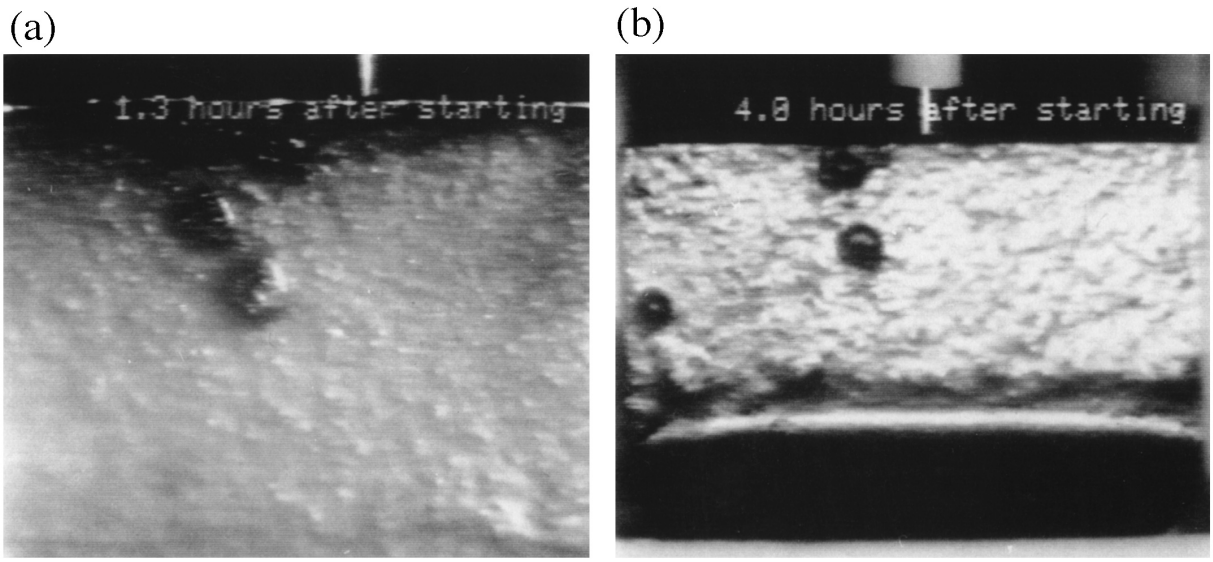

Fig. 7. Surface of non-immersed part of the nickel sheet after: (a) 1 h; (b) 4 h.

After about 120 h, the potential began to shift rapidly to more positive values and reached −40 mV within 1 h. The gas evolution from the surface of the immersed part of the plate became weaker and stopped after the potential reached −44 mV. The potential remained constant at −40 mV while observation continued for 50 h.

To clarify the phenomena which lead up to the non-immersed part of the nickel sheet becoming covered with electrolyte, an advanced test procedure was used for detailed observations. The procedure is basically identical to that described above, but some changes were made in order to facilitate the experiment and the observation. Using the same procedure as previously, observations were made with a new nickel sheet ($25 \times 25 \times 0.25$ mm^3). Photographs of the nickel sheet and electrolyte in the earlier stages of the test are given in Fig. 8. Initially the boundary between the sheet and the electrolyte is sharp. No carbonate film is visible above the meniscus. Some carbonate film is observed above the meniscus after supplying. The area covered by the carbonate film gradually extends to the top of the sheet and is accompanied by gas evolution. After 1 h, the whole sheet is covered with the carbonate film. From this point on, the phenomena observed are the same as in the previous experiment.

Based on these results, the in situ oxidation of the non-immersed part of the nickel sheet may be interpreted as shown in Fig. 9. In a CO_2 atmosphere, very little takes place on the surface. The oxidation process does occur, but at a very slow rate, since the potential corresponds to the equilibrium potential of the nickel-oxidation reaction as shown in Eq. (1). After supplying oxidant gas mixture, the surface is oxidized immediately by oxygen gas, i.e.,

$$Ni + 1/2O_2 = NiO \quad (2)$$

and a thin nickel-oxide layer covers the surface exposed to the gas. The NiO surface is rough and causes carbonate to creep up due to capillary forces. Once the surface is covered by carbonate, the main cathode reaction, Eq. (3), can take place, viz.,

$$CO_2 + 1/2O_2 + 2e^- = CO_3^{2-} \quad (3)$$

Therefore, the nickel-oxidation reaction, Eq. (1), shifts to the right and the oxidation of nickel metal is accelerated. According to the electrochemical theory of corrosion, the potential of the nickel sheet will shift to a more positive value (the corrosion potential) between the equilibrium potentials of reactions (1) and (3).

The gas evolution observed in these experiments follows a complicated pattern that requires a more sophisticated explanation. As long as the non-immersed part of the nickel sheet remains smooth and is covered by a continuous thin electrolyte film, the oxidation of the sheet according to reaction (1) takes place mainly on the immersed part of the sheet, and is accompanied by gas evolution (CO_2). The rate of nickel oxidation on the immersed part is controlled by the reduction of oxygen on the non-immersed part, and is therefore slow. This explains the relatively negative corrosion potential before and during the first plateau. Once the non-immersed surface starts to oxidize and becomes rough, and the electrolyte film is broken up, and gas evolution according to Eq. (1) starts to become vigorous above the meniscus, the oxidation is accelerated. Finally, the oxidation reaction zone extends over the entire upper part of the nickel sheet, which is irregularly covered with carbonate. It is likely that the nickel-oxidation progresses into the sheet as shown in Fig. 9. Finally, the nickel sheet becomes lithiated, as discussed below. From this visual observation, however, it is not clear when the in situ lithiation process takes place [18].

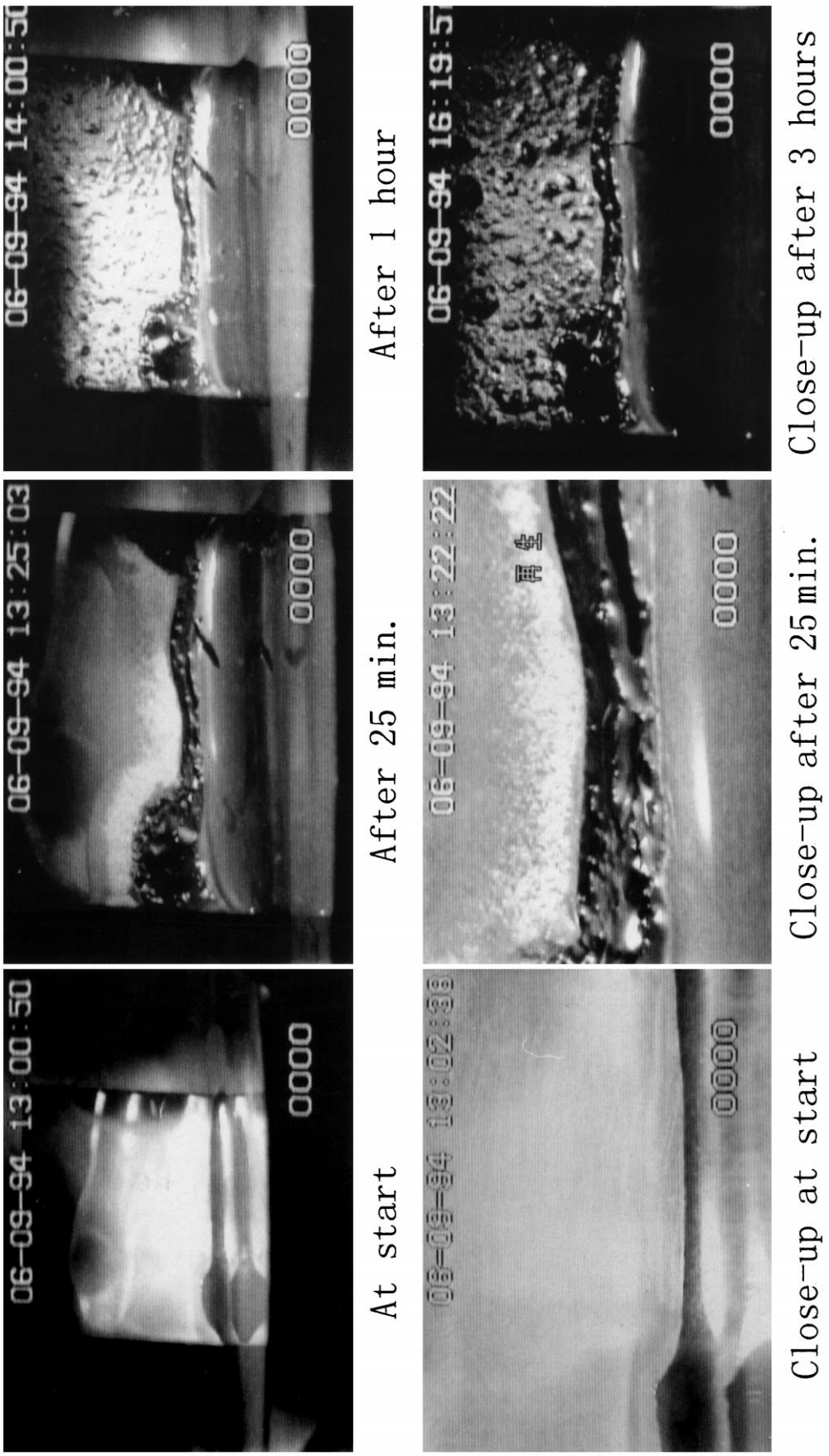

Fig. 8. Photographs of surface of nickel sheet.

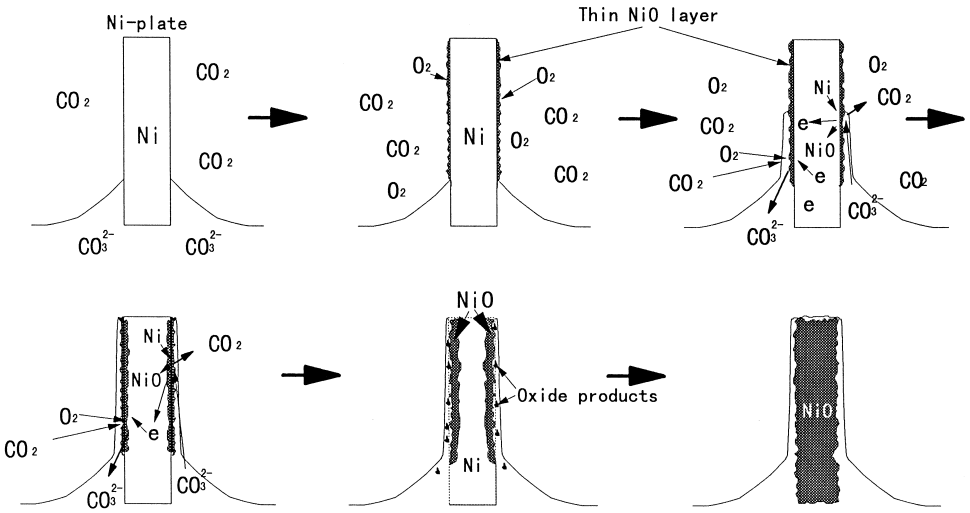

Fig. 9. Schematic diagram of reactions occurring during oxidation of nickel sheet partially immersed in molten carbonate.

3.3. Electrochemical performance of in situ lithiated NiO electrode

After the potential of the nickel sheet shown in Fig. 6 reached the equilibrium value of reaction (3), electrochemical measurements were made in a similar fashion to those for a gold electrode. The potential vs. current characteristics at different immersed depths varying from 5 to 15 mm are shown in Fig. 10. In all cases, there is an almost linear relationship. The influence of immersed depth on these polarization characteristics is only significant at high applied potentials. The current tends to increase with immersion depth, but when the applied potential is less than −300 mV, the effect is weak. This suggests that at potentials more positive than −300 mV, the main reaction zone of the lithiated NiO electrode is the meniscus, i.e., as found previously with a gold electrode. The magnitude of the linear reaction current density is over one order higher than that on the gold electrode. Therefore, the active

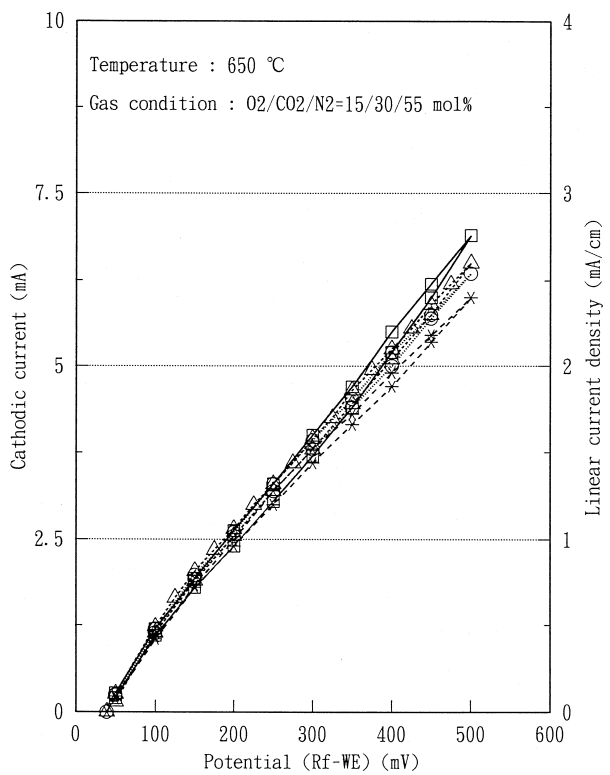

Fig. 10. Effect of immersed depth of nickel cathode on current/potential. Depth: (– □ –) 15 mm; (· · · △ · · ·) 10 mm; (· · · ○ · · ·) 7.5 mm; (– × –) 5 mm.

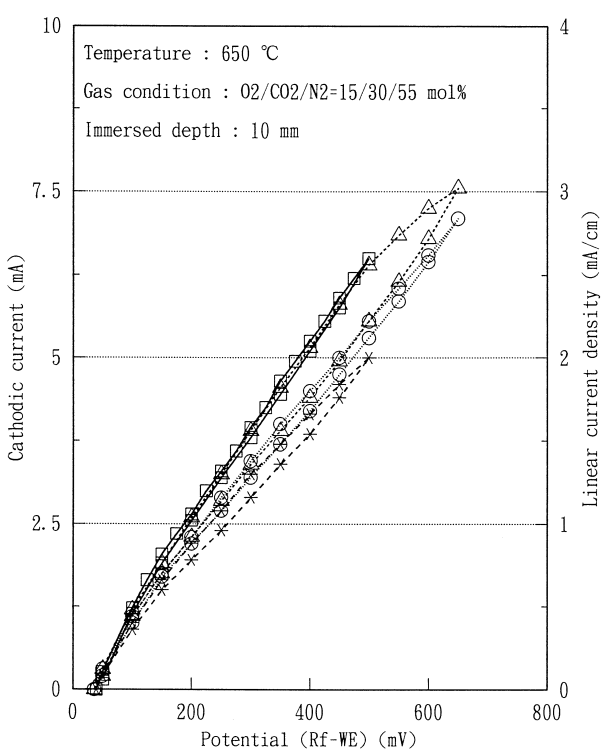

Fig. 11. Effect of elapsed time on polarization of nickel sheet oxidized in situ.

electrode surface of the lithiated NiO appears to be over an order of magnitude larger than the meniscus-reaction zone of the gold electrode.

Fig. 11 shows the polarization characteristics of the same electrode with varying immersion, after extended exposure (up to 167 h) to molten carbonate, at open circuit. The cathodic current at the same polarization potential decreases with time. This means that the lithiation and/or oxidation of the electrode is slow, and continues with time: Note that, the rest potential is also closer to the equilibrium potential.

4. Summary and conclusions

In a pure CO_2 atmosphere, a nickel sheet partially immersed in an eutectic carbonate mixture (Li_2CO_3:K_2CO_3 = 62:38 mol%) is relatively stable. The contact angle measured, by means of direct observation, was similar to that at a gold foil.

In oxidant gas, a change in the surface of the nickel sheet and movement of electrolyte on to the surface are observed, leading ultimately to complete oxidation. The non-immersed part of the nickel sheet gradually becomes covered with carbonate. Intensive electrochemical oxidation with CO_2 gas generation, initially on the immersed part of the metal, takes place during the oxidation-and-lithiation process. Later, the electrochemical oxidation of nickel and reduction of oxygen take place over the entire surface of the foil, until it is oxidized throughout its thickness. This through-oxidation (and lithiation) takes hundreds of hours to complete. Although the oxygen reduction current at the in situ lithiated NiO is over an order of magnitude higher than at the gold electrode, the meniscus and super-meniscus regions still constitute the dominant zone for oxygen reduction in molten carbonate.

The results obtained in this work appear to have important implications for the practice of in situ oxidation/lithiation. Uniform oxidation and lithiation of the particulate nickel structure in the cathode of the MCFC, requires optimum oxygen levels and careful control of temperature and other operation conditions. Depending on the initial size of the nickel particles, the rate of oxidation and the in situ conditions decide the final structure of the cathode and its performance, including wettability. Further studies to explain these phenomena quantitatively may help to establish correlations which are helpful in the design of high-performance cathode structures.

References

[1] M.C. Williams, E.L. Parsons, T.J. George, in: D. Shores, H. Maru, I. Uchida, J.R. Selman (Eds.), Proceedings of the Third International Symposium on Carbonate Fuel Cell Technology, The Electrochemical Society Proceeding Series, Pennington, NJ, 1993, PV 93-3, p. 1.
[2] A. Nakaoka, H. Andou, T. Yoshida, H. Yasue, H. Uematsu, M. Abe, in: Program & Abstracts 1992 Fuel Cell Seminar, pp. 458–461.
[3] L.A.H. Machielse, A.L. Dicks, S. Freni, in: Program & Abstracts 1992 Fuel Cell Seminar, pp. 495–498.
[4] J.R. Selman, H.C. Maru, in: G. Mamantov, J. Braunstein (Eds.), Advances in Molten Salt Chemistry, Vol. 4, Plenum, New York, 1983.
[5] C.D. Iacovangelo, J. Electrochem. Soc. 133 (1986) 2410.
[6] H.R. Kunz, J.W. Pandolf, J. Electrochem. Soc. 139 (1992) 1550.
[7] Y. Mugikura, T. Abe, T. Watanabe, Y. Izaki, Denki Kagaku 60 (1992) 124.
[8] G.M. Moiseev, G.K. Stepanov, in: A.N. Baraboshkin (Ed.), Electrochemistry of Molten and Solid Electrolytes, Vol. 15, Consultants Bureau, New York, 1967 pp. 101–109.
[9] J.M. Fisher, P.S. Bennet, J.F. Pignon, R.C. Makkus, R. Weeuvwer, K. Hemmes, J. Electrochem. Soc. 137 (1990) 1493.
[10] M. Matsumura, J.R. Selman, J. Electrochem. Soc. 139 (1992) 1255.
[11] T. Watanabe, J.R. Selman, in: Program & Abstracts 1992 Fuel Cell Seminar, pp. 559–562.
[12] B.B. Davie, R.E. White, S. Srinivasan, A.J. Appleby, J. Electrochem. Soc. 138 (1991) 673.
[13] S.H. White, U.M. Twardich, J. Electrochem. Soc. 135 (1988) 892.
[14] Y. Mugikura, J.R. Selman, Meniscus behavior of metals and oxides in molten carbonate under oxidation and reducing atmospheres: Part I. Contact angle and electrolyte displacement, J. Electrochem. Soc. 143 (1996) 2442.
[15] G.L. Lee, PhD Dissertation, Illinois Institute of Technology, Chicago, IL, 1993.
[16] Y. Mugikura, J.R. Selman, Denki Kagaku 64 (1996) 491.
[17] V.R. Iyer, O.F. Devereux, J. Electroanal. Chem. 132 (1985) 1098.
[18] T. Nishina, K. Takizawa, I. Uchida, J. Electroanal. Chem. 263 (1989) 87.